Available online at www.sciencedirect.com

ScienceDirect

Procedia Engineering 79 (2014) 386 – 396

Procedia Engineering

www.elsevier.com/locate/procedia

37th National Conference on Theoretical and Applied Mechanics (37th NCTAM 2013) & The 1st International Conference on Mechanics (1st ICM)

Dynamic Analysis of a Rotating Shaft Subject to the Double Cutting Force and Time-Varying Mass Effects of the Rod

W.C. Hsu[a], C.H. Kang[b,*], Y.W. Chen[c], T.N. Shiau[c], D.S. Liu[c]

[a]*Department of Mechanical Engineering, Wu Feng University, Chiayi 621, Taiwan*
[b]*New Energy Division, MAG Technology Co. Ltd, Tainan 717, Taiwan*
[c]*Department of Mechanical Engineering, National Chung Cheng University, Chiayi 621, Taiwan*

Abstract

This paper investigates the dynamic behaviors of a rotating shaft subjected to the double cutting force and time-varying mass effects. The Timoshenko beam theory is used to model the rotating shaft, and the general boundary condition is assumed as the clamped-hinged supports. This system is used to simulate the manufacture process of the double turret CNC lathes, and the mass of the rod which is reduced gradually in cutting process. The system equations of motion are derived based on the global assumed mode method, and the dynamic responses of the system are obtained by Runge-Kutta numerical method. The transformation matrix is derived to make the equation of motion completing the boundary geometric constraints. The numerical results compare the dynamic response in different moving speeds and skew angles of the cutting forces with/without the time-varying mass effects. Additionally, this paper compares the response with single cutting force and double force. The results show that the double moving force system can reduce not only the machining time but also the amplitude of shaft vibration.

Selection and peer-review under responsibility of the National Tsing Hua University, Department of Power Mechanical Engineering

Keywords: rotating shaft, double cutting force, time-varying mass effect;

Nomenclature

A	cross-section area of the shaft
a_i, b_i, c_i, d_i, e_i	coefficients of polynomial
F_U, F_V, F_W	U-dir, V-dir and W-dir force

*Corresponding author. Tel.: +886-6-2664126-348; fax: +886-6-2664983
E-mail address: chkang1977@gmail.com

Selection and peer-review under responsibility of the National Tsing Hua University, Department of Power Mechanical Engineering
doi:10.1016/j.proeng.2014.06.359

E , G	Young's modulus and shear modulus
I	cross-section second moment of area of the shaft
I_d , I_p	diametrical and polar mass moment of inertial of the shaft
k	shear coefficient
L	length of shaft
$[M],[C],[K]$	mass matrix, gyroscopic matrix, and stiffness matrix
N_p	the number of terms of polynomial
$\{q\},\{q_I\}$	generalized coordinates
$[R]$	transformation matrix due to boundary conditions
r	radius of shaft
x_l, x_r	support position of the right side and left side
T_s , U_s	kinetic energy and potential energy of the shaft
(U,V,W)	responses in (X,Y,Z) direction
(B,Γ)	rotations about Y and Z axes
α	non-dimensional moving speed
β	Rayleigh beam coefficient
θ	skew angle of the moving skew force
ρ	density of shaft
$[\Phi(t)]$	time dependent matrix due to axial force
ω	whirl speed
ω_0	fundamental natural frequency of the stationary Euler- Bernoulli beam
Ω , $\bar{\Omega}$	rotating speed and non-dimensional rotational speed

1. Introduction

The double spindle and double turret CNC lathes are generally used presently. Less production time and high economic efficiency are the main advantages of the double turret system. The CNC lathes with double turret system can be applied to multiple processes especially for the cylindrical products. Respecting the above description, the dynamic response of a rotating shaft beam subject to the double moving force is studied in this paper.

The dynamic of the rotating shaft had been analyzed for a long time. Katz at al.[1] presented the study of the dynamic response of a rotating shaft subject to a moving load with constant velocity. The modal analysis and an integral transformation method were employed to obtain the dynamic response. Zu and Han[2] obtained closed-form solutions for the free vibration analysis of spinning Timoshenko beam for the classical boundary conditions. In addition, the dynamic response of a spinning Timoshenko beam with general boundary conditions under the effect of a moving load was also analyzed by Zu and Han[3]. Lee[4] analyzed the dynamic response of the beam with rigid simply supports at the ends and used the vibration modes of a simply supported beam as the assumed functions. The dynamic behaviors of a multi- span Euler-Bernoulli beam on one-sided point constraints was analyzed by using Hamilton's principle and the assumed mode method[5]. Lee also considered the axial nonmoving compressive forces acting on the ends of the shaft and indicated that the effect caused the deflection of the shaft to increase and fluctuate significantly[6]. The dynamic behavior of a shaft subject to a moving deflection dependent load has been studied by Argento[7, 8], Huang and Chang[9]. The load represents the cutting force is varying in the turning process since the workpiece vibrates in the direction of the tool affecting the actual depth of cut. Phan et al.[10] used the finite element method to analyze the static deflection of the workpiece subject to the cutting force in turning, and boundary conditions were clamped-free, clamped-hinged and hinged-hinged. Generally, the FEM[10], Galerkin's method (GM)[7–9], and mode superposition method (MSM)[1–6, 11-13] were employed to analyze the dynamic response of a single-span shaft. The Global Assumed Mode Method (GAMM) proposed by Shiau and Hwang[14] is employed in this paper. The mode shape functions used by GAMM are chosen as a series of polynomial functions.

Shiau et al.[15] introduced the transformation matrix constraining the boundaries of a single-span shaft to force the equations of motion to complete the geometric requirements.

In this paper, the system equation of motion of a rotating shaft is formulated by Lagrangian's approach with the combination of GAMM[14] and the transformation matrix[15] , which is derived to make the equation of motion for completing the boundary constraints.

2. System equations of motion

This paper presents the manufacture system of the shaft as shown in Fig. 1. Fig. 2 shows the configuration and coordinates of a rotating simply supported shaft with double moving cutting load. In this paper, the Timoshenko beam theory is used to model the rotating shaft. As shown in Fig. 2, two reference frames are adopted and they are the Newtonian reference frame $X-Y-Z$ and the rotating reference frame $x-y-z$. Both the X and x axes are collinear and coincident with un-deformed bearing centerline and O is the origin at the middle of the shaft. The rotating frame rotates about the X axis with a whirl speed of ω ; Ω is the rotating speed of the rotor system. F_1 and F_2 are the cutting loads acting on the shaft and θ_1 , θ_2 are the skew angles between Y direction and force directions. The deflections of any cross section of shaft include translations (U,V,W) and rotations (B,Γ). By assumption, the deflections as functions of positions along the rotating axis x and time t can be expressed as:

$$\begin{aligned} &U = U(x,t)\ ,\ \ V = V(x,t)\ ,\ \ W = W(x,t) \\ &\mathrm{B} = \mathrm{B}(x,t),\ \ \Gamma = \Gamma(x,t) \end{aligned} \tag{1}$$

With the GAMM [24], the associated deflections can be rewritten as

$$\begin{aligned} &U(x,t) = \sum_{i=1}^{Np} a_i(t)x^{i-1},\ \ V(x,t) = \sum_{i=1}^{Np} b_i(t)x^{i-1}\ ,\ \ W(x,t) = \sum_{i=1}^{Np} c_i(t)x^{i-1} \\ &\mathrm{B}(x,t) = \sum_{i=1}^{Np} d_i(t)x^{i-1},\ \ \Gamma(x,t) = \sum_{i=1}^{Np} e_i(t)x^{i-1} \end{aligned} \tag{2}$$

where a_i, b_i, c_i,d_i and e_i are time-dependent generalized coordinates, x is the axial location of the shaft, x^{i-1} are the corresponding mode shape functions, and N_p is the number of polynomial terms.

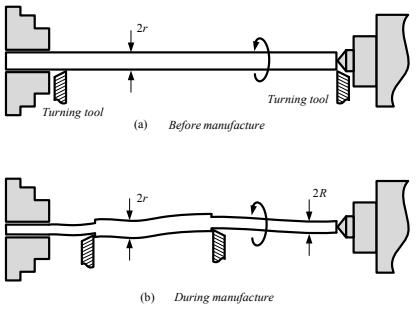

Fig. 1. The manufacture system of the shaft

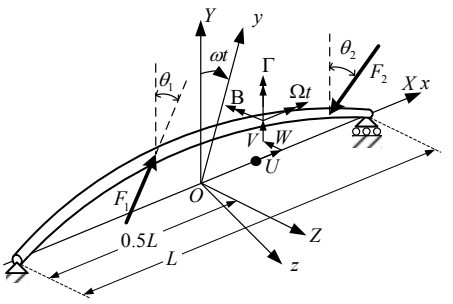

Fig. 2. The coordinates of a rotating shaft with double cutting loads

The derivation for equations of motion using the Lagrangian's approach requires the calculation of the kinetic and potential energy of the system, which can be expressed in terms of the displacements. The kinetic energy T_s and potential energy U_s of the rotating shaft are given by

$$T_s = \frac{1}{2}\int_{x_l}^{x_r} \rho A(\dot{U}^2 + \dot{V}^2 + \dot{W}^2)dx + \frac{1}{2}\int_{x_l}^{x_r} I_d(\dot{\mathrm{B}}^2 + \dot{\Gamma}^2)dx + \frac{1}{2}\int_{x_l}^{x_r} I_p\Omega(\Gamma\dot{\mathrm{B}} - \mathrm{B}\dot{\Gamma})dx + \frac{1}{2}\int_{x_l}^{x_r} I_p\Omega^2 dx \tag{3}$$

$$U_s = \frac{1}{2}\int_{x_l}^{x_r} EA(U')^2 dx + \frac{1}{2}\int_{x_l}^{x_r} EI\{(\mathrm{B}')^2 + (\Gamma')^2\}dx + \frac{1}{2}\int_{x_l}^{x_r} kGA\{(V' - \Gamma)^2 + (W' + \mathrm{B})^2\}dx - \sum_{m=1}^{2}\frac{1}{2}\int_{x_l}^{x_{fm}} F_{m,U}\{(V')^2 + (W')^2\}dx \tag{4}$$

where E is the Young's modulus, k is the shear coefficient, G is the shear modulus, x_r and x_l are the right and left end positions of the shaft, $F_{m,U}$ is the axial component of F_m, x_{f_m} is the position of the cutting load F_m, ρ is the mass density, A is the cross-sectional area of the shaft, I_d and I_p are the diametrical and polar mass moment of inertia, I is the area moment of inertia of shaft. In this paper, at least those five parameters in the above are assumed as time depended in the cutting process, which are changed as the altering of the shaft radius.
The virtual work of the moving force is

$$W_{work} = \sum_{m=1}^{2}(F_{m,V}\delta V_{f_m} + F_{m,W}\delta W_{f_m}) \tag{5}$$

where $F_{m,V}$, $F_{m,W}$ are the components of F_m in Y, Z directions, respectively.
Following the Lagrangian approach, the motion equation of shaft is

$$[M(t)]\{\ddot{q}(t)\} + \Omega[C(t)]\{\dot{q}(t)\} + [K(t) + \Phi(t)]\{q(t)\} = \{F(t)\} \tag{6}$$

Fig. 3 shows the configuration of the shaft with general boundary conditions as clamped-hinged beam conditions. The transformation matrix [15] is applied in this paper for the reason that the shaft does not complete the geometric constraints since the mode shape functions in the above are arbitrary functions. The geometric constraints of the clamped support and hinged support can be expressed as

$$\begin{aligned} &U(x_l,t) = U'(x_l,t) = 0,\ \ V(x_l,t) = V(x_r,t) = V'(x_l,t) = 0, \\ &W(x_l,t) = W(x_r,t) = W'(x_l,t) = 0,\ \ \mathrm{B}'(x_r,t) = \Gamma'(x_r,t) = 0 \end{aligned} \tag{7}$$

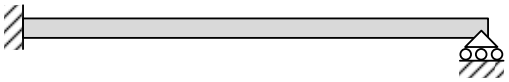

Fig. 3. The configurations of clamped-hinged rotating shaft

Substituting $V(x_l,t) = V(x_r,t) = V'(x_l,t) = 0$, $\mathrm{B}'(x_r,t) = 0$ in Eq. (7) into Eq. (2), the geometric constraint equations for clamped-hinged condition can be expressed as:

$$\{b_1 \quad b_2 \quad \cdots \quad b_{N_p}\}^T = [R_b]\{b_I\},\ \{d_1 \quad d_2 \quad \cdots \quad d_{N_p}\}^T = [R_d]\{d_I\} \tag{8}$$

where

$$\{b_I\} = \{b_3 \quad b_4 \quad \cdots \quad b_{N_p}\}^T,\ \{d_I\} = \{d_1 \quad d_3 \quad d_4 \quad \cdots \quad d_{N_p}\}^T$$

$$[R_b]=\begin{bmatrix} -\begin{bmatrix} 1 & x_l & x_l^2 \\ 1 & x_r & x_r^2 \\ 0 & 1 & 2x_l \end{bmatrix}^{-1}\begin{bmatrix} x_l^3 & x_l^4 & \cdots & x_l^{N_p-1} \\ x_r^3 & x_r^4 & \cdots & x_r^{N_p-1} \\ 3x_l^2 & 4x_l^3 & \cdots & (N_p-1)x_l^{N_p-2} \end{bmatrix} \\ \hline [I] \end{bmatrix},\ [R_d]=\begin{bmatrix} [1] & [0] \\ \hline [0] & \begin{bmatrix} -[2x_r \quad 3x_r^2 \quad \cdots \quad (N_p-1)x_r^{N_p-2}] \\ \hline [I] \end{bmatrix} \end{bmatrix}$$

Base on the above transformation matrix, $[R_b]$ and $[R_d]$ can be obtained by considering the translation (V) and rotation (B) to satisfy each boundary conditions. With the same formulations, the matrices $[R_a]$, $[R_d]$ and $[R_e]$ of each geometrical boundary can also be determined, respectively. The system generalized coordinate vector $\{q\}$ in Eq. (6) can be rewritten as

$$\{q\}=\begin{bmatrix} [R_a] & [0] & [0] & [0] & [0] \\ [0] & [R_b] & [0] & [0] & [0] \\ [0] & [0] & [R_c] & [0] & [0] \\ [0] & [0] & [0] & [R_d] & [0] \\ [0] & [0] & [0] & [0] & [R_e] \end{bmatrix}\begin{Bmatrix} \{a_I\} \\ \{b_I\} \\ \{c_I\} \\ \{d_I\} \\ \{e_I\} \end{Bmatrix}=[R]\{q_I\} \tag{9}$$

And the system equation with associated geometric constraints can be represented as

$$[R]^T[M][R]\{\ddot{q}_I\}+[R]^T\Omega[C][R]\{\dot{q}_I\}+[R]^T[K+\Phi][R]\{q_I\}=[R]^T\{F\} \tag{10}$$

3. Numerical results and discussions

The dynamic response of a rotating shaft with general boundary condition subject to the double constant cutting load is investigated. Some parameters, such as the spin speed of the shaft, the moving velocity, and Rayleigh beam coefficient should be presented and described as the following symbols [6]. $\alpha=v/v_{cr}$ is the non-dimensional moving velocity of the cutting load, where $v_{cr}=(\pi/L)\sqrt{EI/\rho A}$. $\beta=\pi\, r_0/L$ is the Rayleigh beam coefficient for a circular cross section. r_0 is the radius of gyration. $\bar{\Omega}=\Omega/\omega_0$ is the non-dimensional rotational speed, where $\omega_0=(\pi/L)^2\times\sqrt{EI/\rho A}$ is fundamental natural frequency of the stationary Euler- Bernoulli beam. $F=\pi^2\mathrm{EI}/L^2$ is the Euler critical buckling load. U/U_s, V/V_s and W/W_s are the non-dimensional deflections along the shaft due to the moving loads in Y and Z direction, respectively. U_s is the static deflection at the rigid end when the axial force is applied. V_s and W_s are the static deflections as the lateral force is applied at the midpoint of the shaft. The system parameters are considered as Lee[6] and Shiau et al.[15], the actual measurement data are not presented in this paper.

In this paper, the cutting loads are assumed parallel in $X-Y$ plane and move from the end of two sides to the

middle of the shaft. θ_m represents the skew angle between Y and force directions. The material properties and geometric dimensions of the shaft are given as: length $L = 1.0\,m$, density $\rho = 7700\ kg/m^3$, elastic modulus $E = 207\ GPa$, shear modulus $G = 77.6\ GPa$, shear coefficient $k = 0.9$ and radius of the shaft $r = 2\beta L/\pi$ [1, 5]. In the following cases, all the radii of static deflections U_s, V_s, W_s are selected with $\beta = 0.2$. In order to analyse the dynamic response of this system, the numbers of GAMM polynomial terms N_p with clamped-hinged boundary condition are presented for the convergence analysis. In the process of the convergence analysis, the Rayleigh beam coefficient β is selected as 0.03 and rotational speed $\bar{\Omega}$ is selected as 0. Table 1 shows the first three natural frequencies of the rotating shaft beam system with N_p from 8 to 13. Apply the convergence test results in this table, the number of N_p is selected as 12 in this paper. In the following cases, the parameters β, $\bar{\Omega}$ are selected as $\beta = 0.2$, $\bar{\Omega} = 2.5$ and α, θ are selected during $0.5 \le \alpha \le 1.5$, $0^\circ \le \theta \le 60^\circ$. Fig. 4 shows the configurations of the shafts, where r is the radius of the shaft before manufacture, and R is the radius after the manufacture. The abscissas in Fig. 5 and Fig. 6 are the positions of the cutting loads. In those figures, the solid lines mean the cutting load F_1 and the dashed lines mean the cutting load F_2.

Table 1 The natural frequencies of shaft with clamped-hinged boundary condition ($\beta = 0.03$, $\bar{\Omega} = 0$)

	Natural Frequency (*rad/sec*)						
Mode	**1st**	**2nd**	**3rd**	***Mode***	**1st**	**2nd**	**3rd**
N_p=8	760	2448	5203	**N_p=11**	760	2446	5052
N_p=9	760	2447	5061	**N_p=12**	760	2446	5052
N_p=10	760	2446	5057	**N_p=13**	760	2446	5052

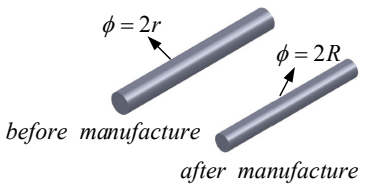

Fig. 4. The configurations of the shafts before and after manufacture

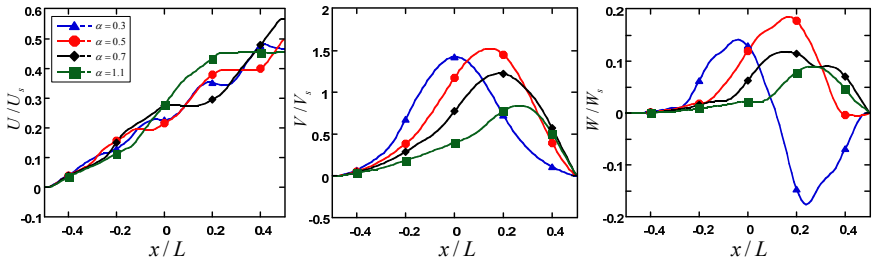

(a) Single cutting force

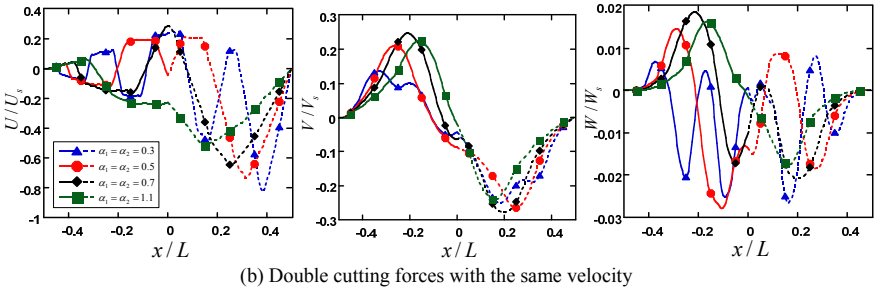

(b) Double cutting forces with the same velocity

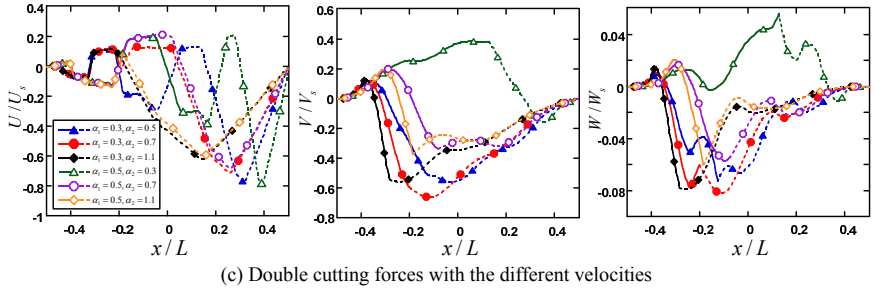

(c) Double cutting forces with the different velocities

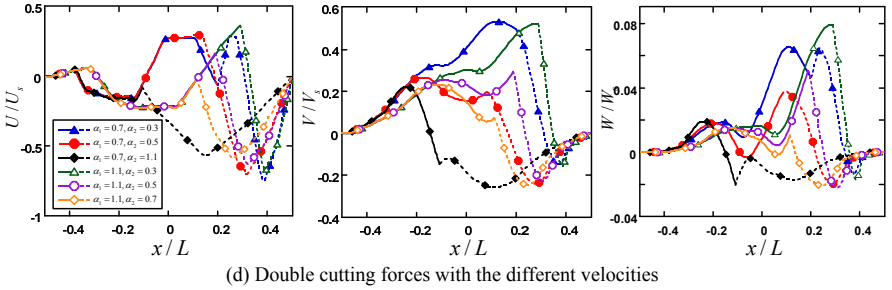

(d) Double cutting forces with the different velocities

Fig. 5. The deflections of the shafts without time-varying mass effects subject to different manufacture velocities ($\beta = 0.2$, $\bar{\Omega} = 2.5$, $\theta = 30^\circ$)

3.1. Dynamic responses without time-varying mass effects

In this case, the time-varying mass effects are not considered temporarily. Both the single cutting load and double cutting load are presented individually. Fig. 5 shows the deflections of the shafts with different manufacture velocities. The skew angles are selected as $\theta_1 = \theta_2 = 30^\circ$. By comparing Fig. 5(a) with Fig. 5(b), the double cutting loads can reduce the deflections in each X , Y and Z directions obviously. As shown in Fig. 5(a) and Fig. 5(b), the change in manufacturing velocities will alter the deflections of shafts, but the deflections are not absolutely proportional directly or inversely to velocities. In Fig. 5(a), the maximum deflection occurs at $\alpha = 0.5$ in Y and Z directions. However, as the shown in Fig. 5(b), the maximum deflection under double forces occurs at $\alpha = 0.3$. In Fig. 5(b), a decrease in manufacture velocity will increase the frequencies of the deflections, which means the

roughness on the shaft surface will be increased at the same time. Fig. 5(c) and Fig. 5(d) show the deflections with different manufacturing velocity combinations. In Fig. 5(c) and Fig. 5(d), most of the deflections in Y and Z directions are positive values if α_1 are larger then α_2. And most of the deflections in Y and Z directions are negative values even though F_1 and F_2 act on the shaft in opposite directions if α_1 are smaller then α_2.

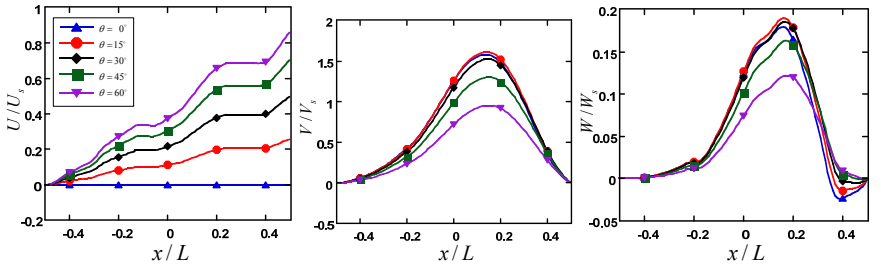

(a) Single cutting force

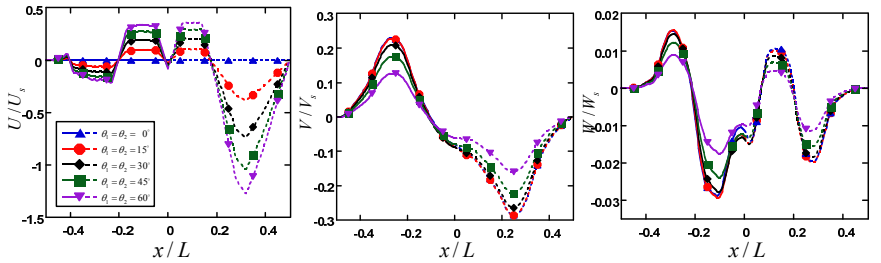

(b) Double cutting forces with the same angle

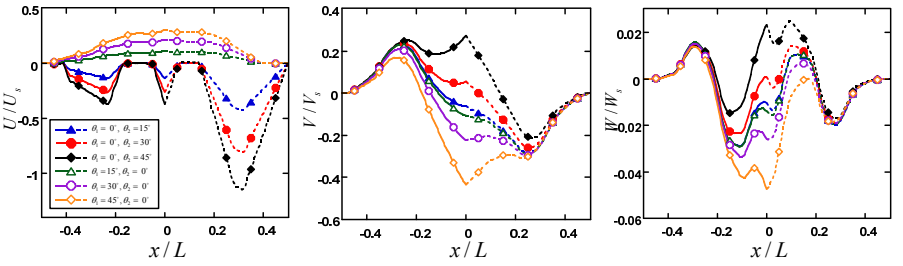

(c) Double cutting forces with different angles

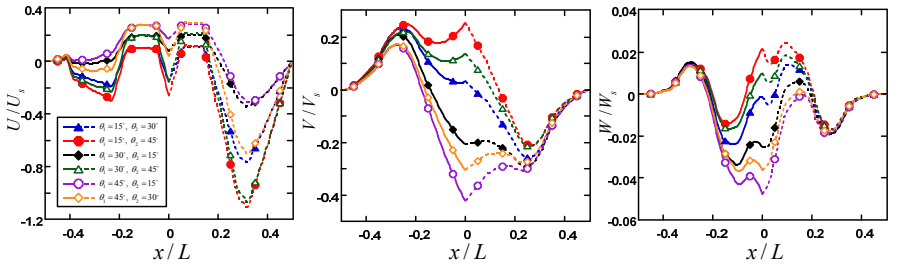

(d) Double cutting forces with different angles

Fig. 6. The deflections of the shafts without time-varying mass effects subjected to different manufacture angles ($\beta = 0.2$, $\bar{\Omega} = 2.5$, $\alpha = 0.5$)

Fig. 6 shows the deflections of shafts under different manufacture angles without time-varying mass effects. In Fig. 6(a) and Fig. 6(b), both the differences of the deflections in Y and Z directions during $0^\circ \le \theta \le 30^\circ$ are unobvious. For the reason that the components of the loadings in Y direction are similar when the skew angles are small, the altering of skew angles just changes the magnitude of the cutting force in Y direction. In Fig. 6(a) and Fig. 6(b), the component of the cutting force in Y direction is decreased with the increase of skew angle. The deflections

in Y and Z directions are decreased at the same time, but situations are opposite in Fig. 6(c) and Fig. 6(d). Fig. 6(c) and Fig. 6(d) show the deflections with different skew angle combinations. When θ_1 keeps the same value, the deflections in each positive directions are increased with the increase of θ_2. When θ_2 keeps the same value, the deflections in each negative directions are increased with the increase of θ_1. The reason is that the restraining effects by the double cutting force are decreased.

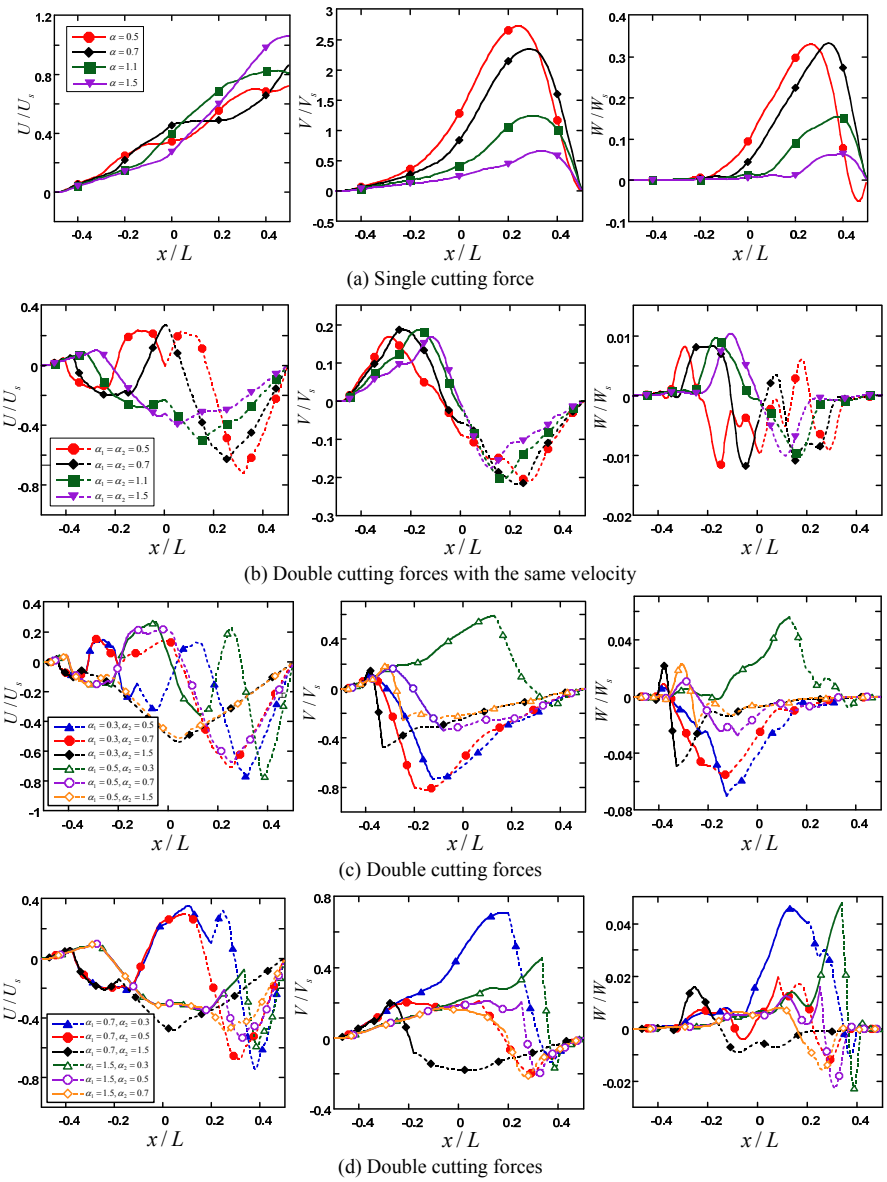

(a) Single cutting force

(b) Double cutting forces with the same velocity

(c) Double cutting forces

(d) Double cutting forces

Fig. 7. The deflections of the shafts with time-varying mass effects subject to different manufacture velocities ($\beta = 0.2$, $\bar{\Omega} = 2.5$, $\theta = 30^{\circ}$)

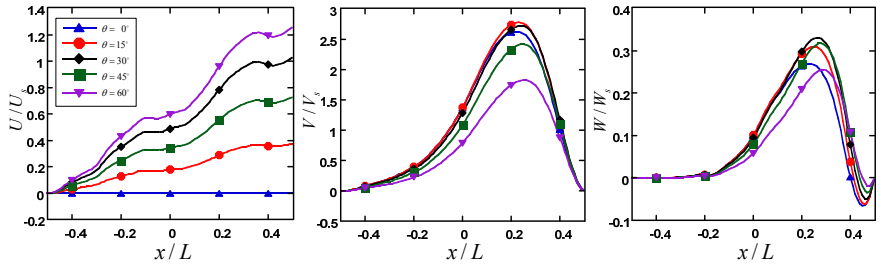

(a) Single cutting force

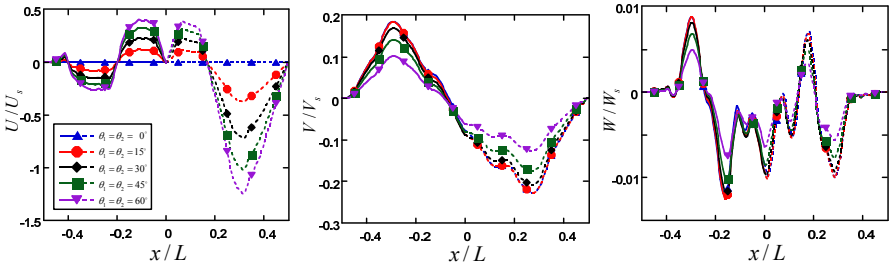

(b) Double cutting forces with the same angle

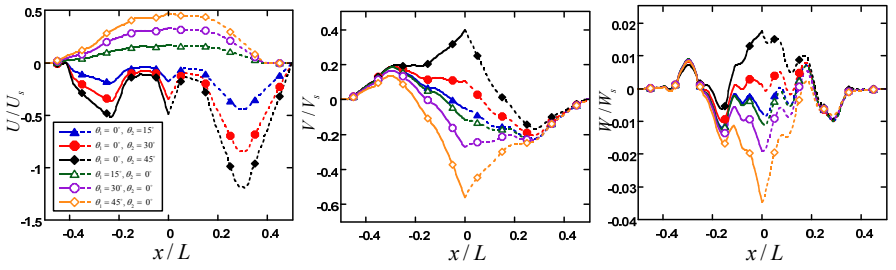

(c) Double cutting forces with different angles

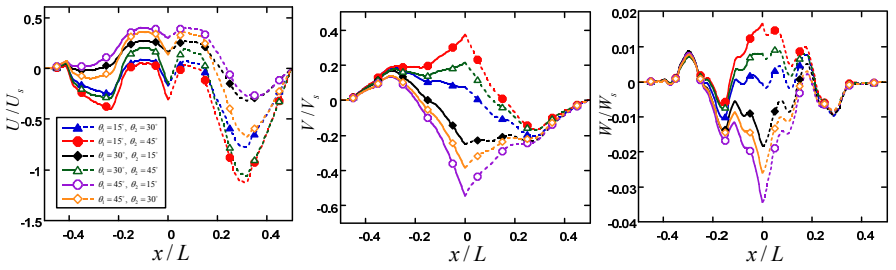

(d) Double cutting forces with different angles

Fig. 8. The deflections of the shafts with time-varying mass effects subject to different manufacture angles ($\beta = 0.2$, $\bar{\Omega} = 2.5$, $\alpha = 0.5$)

3.2. Dynamic responses with time-varying mass effects

The time-varying mass effects are considered in the following cases. In this case, the radius R in Fig. 4 is selected as $0.8r$. Comparing the deflections with/without time-varying effects, the deflections subject to single cutting force in Y and Z directions are increased when the time-varying mass effects are considered. But the deflections subject to double cutting force are decreased when the time-varying mass effects are considered. It means that the restraining effects by the double cutting force are obvious when this mass effects are considered. In Fig. 7(a), the manufacture velocity is the maximum in this case, the deflections have the minimum values. In Fig. 7(b), the deflection in Y direction also has the minimum value when $\alpha = 1.5$, but the deflection in Z direction is the maximum under the same manufacture velocity. Therefore, no matter the time-varying mass effects are

considered or not, the deflections of shafts are not absolutely proportional directly or inversely to manufacture velocity. By comparing with the deflections in Fig. 5(c) and Fig.7(c), the deflections with mass effects in Y direction are larger when $\alpha_1 \neq \alpha_2$, though mass effects are not obvious as the cutting force is single. But the deflections in Z direction are decreased when $\alpha_1 \neq \alpha_2$ such as $\alpha_1 = 0.7$, $\alpha_2 = 0.3$ or $\alpha_1 = 0.7$, $\alpha_2 = 0.5$ under the mass effects are considered. Comparing Fig. 7(c) with Fig. 7(d), the deflections of the left side for the shaft are close during the initial manufacture process when α_1 is large, but this situation is not obvious when α_2 is small.

Fig. 8 shows the deflections of shafts under different manufacture angles with the mass effects. As shown in Fig. 8(a) and Fig. 8(b), the deflections are increased when the time-varying mass effects are considered. But the deflections in Z direction are decreased, as shown in Fig. 8(c) and Fig. 8(d), when the mass effects are considered under $\theta_1 \neq \theta_2$. The effects of skew angle are small when the cutting forces are close to vertical of the shaft. As the shown in Fig. 6 and Fig. 8, the deflections of the shaft are close during the initial manufacture process when different skew angle combinations are presented, no matter the time-varying mass effects are considered or not.

4. Conclusions

In this paper, the dynamic behaviors of a rotating shaft subject to the double moving force and time-varying mass effects are analyzed to simulate machining process of the double turret CNC lathes. The mass of the rod is reduced gradually during cutting process. The transformation matrix based on global assumed mode method is proposed to derive the equation of motion for this system under boundary geometric constraints. Varying manufacture velocity will change the deflections of the shaft, but deflections are not absolute proportional directly or inversely to velocity when the manufacture is under the double cutting force. The deflections of the shaft subject to the single cutting force are increased when the time-varying mass effects are considered, but they are decreased as this shaft is manufactured under the double cutting force. It means that the deflections of the shaft can be decreased effectively by considering the double cutting force, especially when the time-varying mass effects are considered.

References

[1] Katz, R., Lee, C.W., Ulsoy, A.G., Scott, R.A., 1988. The dynamic response of a rotating shaft subject to a moving load, J. Sound Vibr. 122, p.131.
[2] Zu, J.W.Z., Han, R.P.S, 1992. Natural frequency and normal modes of a spinning Timoshenko beam with general boundary conditions, J. Appl. Mech-T ASME 59, p.197.
[3] Zu, J.W.Z., Han, R.P.S, 1994. Dynamic response of a spinning Timoshenko beam with general boundary conditions and subject to a moving load, J. Appl. Mech-T ASME 61, p.152.
[4] Lee, H.P., 1994. Dynamic response of a beam with intermediate point constraints subject to a moving load, J. Sound Vibr. 171, p.361.
[5] Lee, H.P., 1995. Dynamic response of a multi-span beam on one-sided point constraints subject to a moving load, Comput. Struct. 55, p.615.
[6] Lee, H.P., 1995. Dynamic response of a rotating Timoshenko shaft subject to axial forces and moving loads, J. Sound Vibr. 181, p.169.
[7] Argento, A., 1995. A spinning beam subjected to a moving deflection dependent load, part I: response and resonance, J. Sound Vibr. 182, p.595.
[8] Argento, A., Morano, H.L., 1995. A spinning beam subjected to a moving deflection dependent load, part II: parametric resonance, J. Sound Vibr.182, p.617.
[9] Huang, Y.M., Chang, K.K., 1997. Stability analysis of a rotating beam under a moving motion-dependent force, J. Sound Vibr.202, p.427.
[10] Phan, A-V, Cloutier, G., Mayer, J.R.R., 1999. A finite element model with closed-form solutions to workpiece deflections in turning, Int. J. Prod. Res. 37, p.4039.
[11] Yuan, L., Järvenpää, V.M., Keskinen, E., Cotsaftis, M., 2002. Simulation of roll grinding system dynamics with rotor equations and speed control, Commun. Nonlinear Sci. Numer. Simulat. 7, p.95.
[12] Guo, J., Han, R., 2006. A united model of diameter error in slender bar turning with a follower Rest, Int. J. Mach. Tools Manuf. 46, p.1002.
[13] Ouyang, H., Wang, M., 2007. Dynamics of a rotating shaft subject to a three- directional moving load, J. Vib. Acoust. 129, p.386.
[14] Shiau, T.N., Hwang, J.L., 1989. A new approach to the dynamic characteristic of undamped rotor-bearing systems, J. Vib. Acoust. 111, p.379.
[15] Shiau, T.N., Huang, K.H., Wang, F.C., Hsu, W.C., 2009. Dynamic response of a rotating multi-span shaft with general boundary conditions subjected to a moving load, J. Sound Vibr. 323, p.1045.